Drug Design, Development and Therapy

Dovepress
open access to scientific and medical research

Open Access Full Text Article

ORIGINAL RESEARCH

Chondroprotective Mechanism of *Eucommia ulmoides* Oliv.-*Glycyrrhiza uralensis* Fisch. Couplet Medicines in Knee Osteoarthritis via Experimental Study and Network Pharmacology Analysis

Pinger Wang[1–3,*], Jianbo Xu[1,*], Qi Sun[4,*], Qinwen Ge[2,3], Min Qiu[1], Kaiao Zou[2,3], Jun Ying[3,5], Wenhua Yuan[2,3], Jiali Chen[2,3], Qinghe Zeng[2,3], Qi Cui[1], Hongting Jin[2,3], Chunchun Zhang[1], Fanzhu Li[1]

[1]College of Pharmaceutical Sciences, Zhejiang Chinese Medical University, Hangzhou, People's Republic of China; [2]Institute of Orthopaedics and Traumatology, The First Affiliated Hospital of Zhejiang Chinese Medical University, Hangzhou, People's Republic of China; [3]The First College of Clinical Medicine, Zhejiang Chinese Medical University, Hangzhou, People's Republic of China; [4]Department of Orthopedic Joint Surgery, Hangzhou Fuyang Hospital of TCM Orthopaedics and Traumatology, Hangzhou, People's Republic of China; [5]Department of Orthopedic Surgery, the First Affiliated Hospital of Zhejiang Chinese Medical University, Hangzhou, People's Republic of China

*These authors contributed equally to this work

Correspondence: Chunchun Zhang, College of Pharmaceutical Sciences, Zhejiang Chinese Medical University, Hangzhou, Zhejiang, 310053, People's Republic of China, Tel/Fax +86 571-86613684, Email 20081026@zcmu.edu.cn; Fanzhu Li, College of Pharmaceutical Sciences, Zhejiang Chinese Medical University, Hangzhou, Zhejiang, 310053, People's Republic of China, Tel/Fax +86 571-86613684, Email lifanzhu@zcmu.edu.cn

Background: Knee osteoarthritis (KOA) is the primary prevalent disabling joint disorder among osteoarthritis (OA), and there is no particularly effective treatment at the clinic. Traditional Chinese medicine (TCM) herbs, such as *Eucommia ulmoides* Oliv. and *Glycyrrhiza uralensis* Fisch. (E.G.) couplet medicines, have been reported to exhibit beneficial health effects on KOA, exact mechanism of E.G. nevertheless is not fully elucidated.

Purpose: We assess the therapeutic effects of E.G. on KOA and explore its underlying molecular mechanism.

Methods: UPLC-Q-TOF/MS technique was used to analyze the active chemical constituents of E.G. The destabilization of the medial meniscus model (DMM) was employed to evaluate the chondroprotective action of E.G. in KOA mice using histomorphometry, μCT, behavioral testing and immunohistochemical staining. Additionally, network pharmacology and molecular docking were used to predict potential targets for anti-KOA activities of E.G., which was further verified through in vitro experiments.

Results: In vivo studies have shown that E.G. could significantly ameliorate DMM-induced KOA phenotypes including subchondral bone sclerosis, cartilage degradation, gait abnormality and thermal pain reaction sensibility. E.G. treatment could also promote extracellular matrix synthesis to protect articular chondrocytes, which was indicated by Col2 and Aggrecan expressions, as well as reducing matrix degradation by inhibiting MMP13 expression. Interestingly, network pharmacologic analysis showed that PPARG might be a therapeutic center. Further study proved that E.G.-containing serum (EGS) could up-regulate *PPARG* mRNA level in IL-1β-induced chondrocytes. Notably, significant effects of EGS on the increment of anabolic gene expressions (*Col2, Aggrecan*) and the decrement of catabolic gene expressions (*MMP13, Adamts5*) in KOA chondrocytes were abolished due to the silence of *PPARG*.

Conclusion: E.G. played a chondroprotective role in anti-KOA by inhibiting extracellular matrix degradation, which might be related to PPARG.

Keywords: couplet medicines, UPLC-Q-TOF/MS, network pharmacology, cartilage degeneration, knee osteoarthritis, PPARG

Introduction

Osteoarthritis (OA) is the most common degenerative disease, characterized by subchondral bone sclerosis, cartilage degeneration, synovitis and inflammation of joints.[1] Estimated 250 million individuals worldwide are affected by OA.[2,3] Knee osteoarthritis (KOA) is the most common form of disabling joint disease. According to the epidemiological studies, KOA prevalence is found to be 16%, 2.1-fold higher since the mid-20th century.[4] Although many risk factors have been identified, including

Received: 11 November 2022
Accepted: 7 February 2023
Published: 27 February 2023

Graphical Abstract

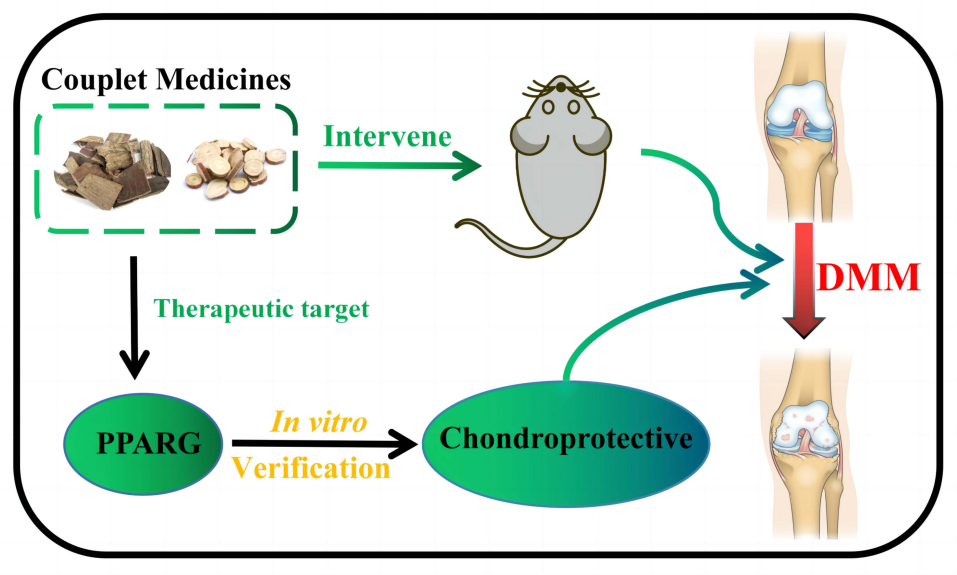

mechanical loading, aging, genetic inheritance and metabolic alterations, it is important for local-low grade inflammation to jeopardize cartilage destruction leading to KOA.[5–7] Studies have identified that pro-inflammatory cytokines, like interleukin (IL)-1β, have driven catabolic degradative enzymes production leading to osteoarthritis cartilage extracellular matrix degradation. In the knee joint, 95% of hyaline cartilage is composed of extracellular matrix, which could provide a stable structural foundation for ensuring the integrity of cartilage.[8–10]

Clinically, there is no efficient disease-modifying treatment except nonsteroidal antiinflammatory drugs (NSAIDs) are normally utilized to relieve pain, which has long-term side effects on gastrointestinal and cerebrovascular diseases.[11,12] As a consequence, knee replacement surgery becomes the ultimately therapeutic option for patients with OA.[13–15] Accordingly, there is an extreme public health urgency to develop safer and more effective therapies for KOA.

Traditional Chinese medicine (TCM) has been shown to be remarkably effective for treating KOA in clinics. According to previous studies, the aqueous extract of *Eucommia ulmoides* Oliv. has the effects of strengthening muscles and bones, improving the quality of osteological mechanics.[16,17] The Chinese herb *Glycyrrhiza uralensis* Fisch. has been effectively used in clinical practice due to its anti-inflammatory effect.[18,19] In many classic KOA treatments, including Duhuo Jisheng formula and Bushen Huoxue decoction,[20–23] *Eucommia ulmoides* Oliv. and *Glycyrrhiza uralensis* Fisch. play crucial roles. In addition, *Glycyrrhiza uralensis* Fisch. is often paired with other herbs, and its active compounds can reversibly bind to other herbal active ingredients, prolonging their release time in the body and enhancing their potential. Hence, *Eucommia ulmoides* Oliv. and *Glycyrrhiza uralensis* Fisch. (E.G.) couplet medicines may play a synergistic enhancement effect in the treatment of KOA. Nevertheless, the effective constituent of E.G. and its potential mechanisms of E.G. against KOA remain unclear.

In the present study, ultra performance liquid chromatography and quadrupole/time-of-flight mass spectrometry (UPLC-Q-TOF/MS) untargeted metabolomics analysis were used to distinguish the main active ingredients of E.G. The effects of E.G. against KOA were investigated in vitro and in vivo. Additionally, network pharmacology analysis and verified experiments facilitate to comprehensively understand the medicinal value of E.G., especially its targets and mechanism in treating KOA.

Materials and Methods

Materials

Eucommia ulmoides Oliv. and *Glycyrrhiza uralensis* Fisch. were purchased from Zhejiang Chinese Medical University Chinese Herbal Pieces Co., Ltd. (Hangzhou, China) (lot. No. 210201). The identification of the two herbs used in this study was undertaken

by Zhejiang Chinese Medical University Chinese Herbal Pieces Co., Ltd. on the basis of the Chinese Pharmacopeia (2020, Edition). According to the ratio in the prescription, the drug was finally prepared into 630 g/L and stored in aliquots at −20 °C until use. For untargeted metabolomics analysis of E.G., the extraction solution was diluted with methanol to 10 mg/mL and centrifuged (4 °C, 12,000 g, and 10 min) to obtain the supernatant. The supernatant was filtered through a microporous membrane filter of 0.22 μm in diameter. Prior to analysis, the sample was stored at 4 °C.

UPLC-Q-TOF/MS

An ultra-performance liquid chromatography and quadrupole/time-of-flight mass spectrometry system were utilized to analyze the samples. First, the UPLC system with a Waters C18 (2.1 mm × 100 mm, 1.7 μm particle size) was utilized to separate the components. The flow rate and temperature were 0.3mL/min and 35 °C, respectively. The gradient elution conditions were as follows: Table S1. The tandem quadrupole time-of-flight mass spectrometry was utilized to detect the components separated by UPLC. Then, data analysis is carried out using UNIFI V1.8 software. All the parameter conditions for mass spectrometry are presented in Table S2.

Mice

We used 10-week-old C57BL/6 male mice purchased from Hangzhou Medical College (Certificate number: SCXK (Zhe) 2019–0002) and kept them at the Experimental Animal Center of Zhejiang Chinese Medical University (Certificate number: SYXK (Zhe) 2021–0012). The mice in this study were kept in pathogen-free cages with a 12-h light/dark cycle and were free to access food and water. The Animal Care and Ethics Committee of Zhejiang Chinese Medical University approved all animal experiments, and as per regulations of the Chinese Ministry of Science and Technology.

Osteoarthritic Model

Based on previous reports, we used an experimental model with surgical destabilization of the medial meniscus (DMM), which exhibits severe cartilage degradation and cartilage damage characteristic of OA.[24] The medial meniscus tibial ligament of C57BL/6 mice was made unstable during DMM surgery. In the sham group, no joint tissue was manipulated during surgery. We divided the mice into five groups at random: Sham group; DMM group; E.G. low group (E.G. L group); E.G. medium group (E.G. M group) and E.G. high group (E.G. H group). According to animal dose conversion table, we then determined the dose of the experimental group. After OA modeling, mice in E.G. high group received E.G. treatment at a dose of 1.17 g/kg/day orally for 12 consecutive weeks. Ratio of high, medium and low-dose groups is 4:2:1. Physiological saline was administered orally to mice in both the sham and DMM groups.

Gait Analysis and Hot Plate Test

At twelfth week after treatment, a DigGait Imaging System (Mouse Specifics, Boston, MA, USA) was utilized to follow and analyze the mice's gait. The mice were placed on a transparent treadmill belt and ran at a speed of 18 cm/second. The 2-dimensional stride characteristics of their limbs were seized by a video recorder. A high-speed (148 frames/s) color video camera in ventral view was utilized to capture the images. Sequential strides determined by the area of the paws for each of the four limbs were necessary for determination of spatial and kinematic indices. Stride length (cm), paw area (cm^2) and swing (s) were calculated to analyze the strides of the right hind. Pain levels in mice were assessed by the hot plate method. After 2 h of gavage, mice were again placed on a surface at 50 ± 0.1 °C and their movements were restricted with plexiglass cylinders. The reaction interval time between reaching the platform surface and the reaction instigated was recognized as the response latency. Reaction behavior consisted of hind leg flinching, paw licking and jumping.

2.6 μCT Analysis

The right knee joints of all mice were collected and fixed in 4% paraformaldehyde for 3 days at week 12 post-operation. In the next step, these tissues were placed in 70% ethanol and then analyzed with a micro-computed tomography (μCT) (Skyscan 1276, Bruker, Kontich, Belgium) at a resolution of 11 mm per pixel, a voltage of 55k, and a current of 200 milliamps. NRecon (v1.7.4.6) was utilized to reconstruct the scanned images. CTAn (v1.20) was utilized to analyze parameters of trabecular bone

in metaphysis. CTvol (v2.0) and CTvox (v3.3) were utilized to perform a three-dimensional model visualization of knee joints. 3D histomorphometric analysis was performed on the medial compartment of the tibial subchondral bone.

Histochemistry, Immunohistochemistry and Histomorphometry

For 14 days, the knee joints were decalcified in 14% ethylenediamine tetraacetic acid solution after μCT analysis, embedded in paraffin and prepared as 4 μm thick sections as described in the literature.[25] The paraffin sections were stained with Toluidine Blue staining (TB) and Alcian Blue Hematoxylin/Orange G staining (ABH) to determine the tissue structure of the knee joint. The thickness and wear degree of knee cartilage were analyzed using OsteoMetrics software (Decatur, GA, USA). Expressions of Collagen Type II (Col2), matrix metalloproteinase 13 (MMP13), Aggrecan, and peroxisome proliferator-activated receptor gamma (PPARG) were observed using immunohistochemistry. Immunohistochemical staining was performed regarding previous literature reports.[26] Anti-Col2 (Abcam, ab34712, 1:200), anti-MMP13 (Abcam, ab39012, 1:100), anti-Aggrecan (Bioss, bs-11655R, 1:200) and anti-PPARG (Arigo, ARG55241, 1:200) were utilized in this study. MMP13 and PPARG expression were counted by the percentage of positively stained cells to total chondrocytes in the region of interest. By counting the positive stained area in the region of interest, Col2 expression was quantified.

Cell Isolation and Culture

The 2-week-old C57BL/6 mice were utilized to isolate primary chondrocytes. After euthanasia, mice were sterilized in 70% ethanol for 5–10 min. Following this, the femoral head cartilages were removed from mice using forceps and cut into pieces. Immediately, these cartilage pieces were washed four times with pre-cold PBS and transferred to a 10 cm petri-dish, digested with 10 mL digest medium (DMEM, 10% FBS, 1% penicillin-streptomycin, 1% L-Glutamine, 0.25 mg/mL Collagenase P) in a 37 °C incubator for 6 h. During digestion, these cartilage tissues were blown 30–40 times with a pipette every 1 h. Then, the digested cells were filtered with 70 μm cell strainers (Corning Falcon 352350), centrifuged at 400 g for 5 min, and cultivated in a medium (DMEM, 10% FBS, 1% penicillin-streptomycin, 1% L-Glutamine).

E.G-Containing Serum (EGS) Preparation and Cellular Experiment

Twenty 10-week-old Sprague Dawley (SD) rats were randomly split into E.G. group and control group. Rats in E. G. group or control group were used to prepare E.G.-containing serum (EGS) or control serum (CS) via oral administration of E.G. (1.17 g/kg/day) or physiological saline for consecutively 7 days. To obtain EGS and CS, blood samples were collected 2 h after the last administration and centrifuged for 15 min at 3000 rpm. In order to prolong the shelf life of EGS and CS, both were sterilized via 0.22 μm filter membranes, subpackaged and stored at −80 °C. For cellular experiment, primary chondrocytes were divided into nine groups: 10% CS, 10% CS+IL-1β, 10% EGS+IL-1β, 20% CS, 20% CS+IL-1β, 20% EGS+IL-1β, 40% CS, 40% CS+IL-1β, 40% EGS+IL-1β. Different concentrations of EGS, CS and IL-1β (10 ng/mL) were co-treated with chondrocytes for 24 h.

siRNA Transfection

The small interfering RNA (siRNA) sequence of *PPARG* gene was designed and synthesized by Shanghai Jima Pharmaceutical Technology Co., LTD. *PPARG* siRNA was transformed into primary chondrocytes by using X-tremeGENE™ siRNA Transfection Reagent (Roche, Mannheim, Germany) according to the manufacturing procedure. Fresh medium (DMEM, 10% FBS, 1% L-Glutamine) was replaced by 6 h after transfection, and cells were collected or processed 48 h after transfection. Real-time PCR was used to measure the expression of *PPARG* mRNA in chondrocytes and the interference efficiency of *PPARG* siRNA.

Real-Time PCR

Total RNA was removed with RNAiso Plus (Takara, Japan). PrimeScript^{TM} RT Reagent Kit (Takara, Japan) was used for reverse transcription reactions. Real-time PCR was conducted with 2 × SYBR Green qPCR Master Mix (Low ROX) reagent (Bimake, China). The relative expression levels of target genes were calculated using the $2^{-\Delta\Delta}$CT method and normalized by β-actin. The primer sequence of the target gene is reproduced below Table 1.

Table 1 Primer Sequences for Quantitative Real-Time PCR

Gene Name	Forward Primers (5'-3')	Reverse Primers (5'-3')
Col2a1	GCTGGTGAAGAAGGCAAACGAG	CCATCTTGACCTGGGAATCCAC
Mmp13	GATGACCTGTCTGAGGAAGACC	GCATTTCTCGGAGCCTGTCAAC
Aggrecan	CAGGCTATGAGCAGTGTGATGC	GCTGCTGTCTTTGTCACCCACA
Adamts5	CTGCCTTCAAGGCAAATGTGTGG	CAATGGCGGTAGGCAAACTGCA
Pparg	GTACTGTCGGTTTCAGAAGTGCC	ATCTCCGCCAACAGCTTCTCCT
β-actin	CATTGCTGACAGGATGCAGAAGG	TGCTGGAAGGTGGACAGTGAGG

Network Pharmacological Analysis

TCMSP database was searched for E.G. compounds with oral bioavailability (OB) of 30% and drug-likeness (DL) of 0.18. To identify potential target proteins, we searched the UniProt databases with the delimited conditions of "Homo sapiens" and "reviewed." The key word "knee osteoarthritis" was imported to GeneCards, OMIM, PharmGkb, TTD and DrugBank to acquire knee osteoarthritis-related targets, among which repetitions were removed. The targets collected above were converted to official gene symbols by the UniProt database, and the Component-Target network of Couplet Medicines was created by Cytoscape 3.8.0. Couplet Medicines against KOA may target bioactive compounds and KOA as common targets. Through STRING's website, these common targets were uploaded to form the PPI network. It was limited to "Homo sapiens" and the confidence score was over 0.96.

DAVID database was used to perform Gene Ontology (GO) and Kyoto Encyclopaedia of Genes and Genomes (KEGG) enrichment analyses for identified common targets. GO analysis and KEGG analysis recognized biological progresses (BPs) and pathways as statistically significant based on $P<0.05$.

Molecular Docking

ChemBio3D (14.0.0.117) was used to convert 2D chemical structures to 3D structures and save them in MOL2 format from PubChem Compound. Target crystal structures were obtained from the RCSB Protein Data Bank. Singly one protein target, peroxisome proliferative activated receptor, gamma (PPARG, PDB ID:2VV4), was investigated. AutoDockTools 1.5.6 was used to convert receptors and ligands from their native formats to pdbqt formats. By deleting water molecules and adding hydrogen atoms, structures were optimized. Then, molecular docking study was performed utilizing Autodock Vina. All docking run options were set to default values according to the Genetic Algorithm. Using PyMoL, the docking results with the highest scores were visualized.

Statistical Analysis

The data were presented as meaning ± standard deviation. Statistically significant differences were defined as those with P values less than 0.05 in a one-way analysis of variance (ANOVA). Statistics were analyzed using SPSS 25.0.

Results

Identification of Active Ingredients in E.G

Under UPLC-Q-TOF/MS analyses, the active ingredients of E.G. were confirmed responsibly. As shown in Figure 1, E. G. was chromatographed in a positive ion mode using total ion chromatography. By comparing retention time, response value and published literature with the reference standard, our primary screen identified 15 compounds, such as beta-Glycyrrhetinic acid, liquiritin, (+)-Pinoresinol-di-O-β-D-glucoside and Geniposidic acid (Table 2).

E.G Decelerated the KOA Progression in DMM-Induced Osteoarthritic Mice

To investigate the effect of E.G. on KOA progression, we established osteoarthritis model mice through DMM surgery. In the DMM-induced mice, prominent damage was seen to the articular cartilage, as well as a reduction in cartilage area and thickness (Figure 2A–C). These histological findings were confirmed by OARSI scoring of cartilage damage in mice, with significantly higher scores in the DMM group than in the sham group (Figure 2D). While E.G. group mice displayed

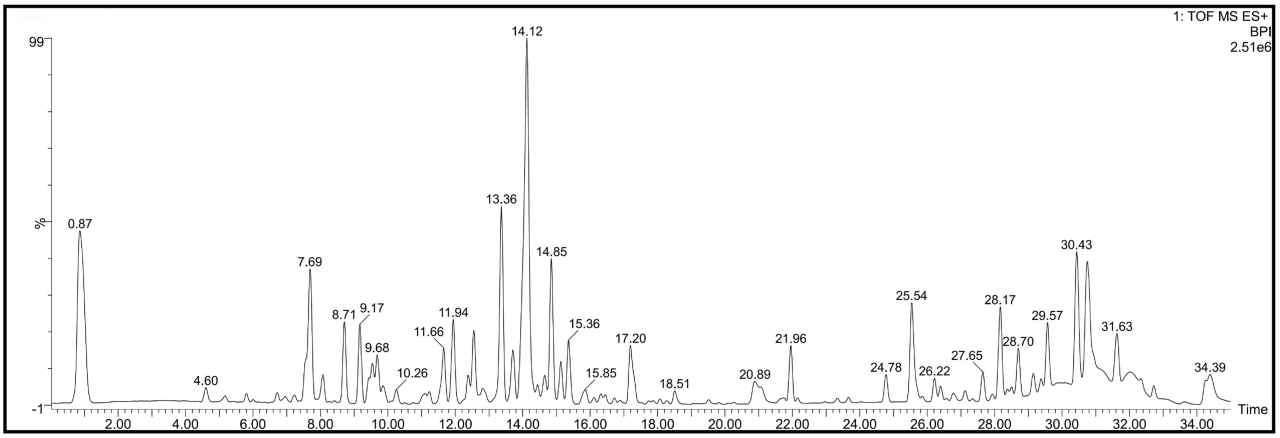

Figure 1 The total ion chromatogram of E.G in positive ion modes.

more intact cartilage tissue with improvement of cartilage area, cartilage thickness and lower OARSI score in a dose-dependent manner (Figure 2). Additionally, μCT was utilized to examine subchondral bone microarchitecture and osteophyte formation. Results showed that the number of osteophytes and BV/TV, Tb.Th measurements of subchondral bone in the DMM group were significantly higher than in sham group mice. After 12-week treatment with E.G., the perpendicular osteophytes and BV/TV, Tb.Th in subchondral bone were dramatically inhibited compared with DMM group (Figure 2E–G). Taken together, DMM-induced KOA mice were protected from cartilage degradation and subchondral bone sclerosis by E.G. treatment.

E.G Alleviated Behavioural Pathological Changes and Pain in the DMM-Induced KOA Mice

Depending on previous reports, gait and analgesic activity in DMM-induced KOA mice is altered due to knee pain and dysfunction. In the current study, gait analysis and hot-plate test were used in determining whether E.G. could relieve the symptoms of DMM-induced KOA mice. As shown in Figure 3, mice in the DMM group exhibited decreasing stride length, paw area and hot plate reaction time and increasing swing time compared with the sham group, and E.G. dose-

Table 2 The Detailed Information of Active Ingredients Contained in E.G

Component Name	Chemical Formula	Observation Retention Time (Min)	Molecular Mass Number (Da)	Observed m/z	Detector Count	Response Value	Additives
Aucubin	$C_{15}H_{22}O_9$	1.55	346.12638	369.1151	4951	3994	+Na, +K
Geniposidic acid	$C_{16}H_{22}O_{10}$	2.84	374.1213	397.1099	66,645	7287	+Na, +H
(+)-Pinoresinol-di-O-β-D-glucoside	$C_{32}H_{42}O_{16}$	6.72	682.24729	705.2369	136,238	11,100	+Na, +H, +K
Pinocembrin	$C_{15}H_{12}O_4$	7.7	256.07356	257.0808	928,235	666,919	+H
Naringenin	$C_{15}H_{12}O_5$	8.81	272.06847	273.0747	19,411	15,765	+H
Liquiritin	$C_{21}H_{22}O_9$	9.7	418.12638	419.1335	151,886	114,597	+H, +Na
Liquiritigenin	$C_{15}H_{12}O_4$	10.25	256.07356	257.0797	84,205	67,748	+H
Isoglabrolide	$C_{30}H_{44}O_4$	12.55	468.32396	469.3313	740,402	511,085	+H
Licorice-saponin G2	$C_{42}H_{62}O_{17}$	13.37	838.3987	839.4086	3,490,036	1,777,493	+H, +Na, +K
Glycyrol	$C_{21}H_{18}O_6$	14.59	366.11034	367.1163	7856	1011	+H
Kaempferol	$C_{15}H_{10}O_6$	16.45	286.04774	287.0546	2647	2270	+H
Semilicoisoflavone B	$C_{20}H_{16}O_6$	18.51	352.09469	353.1013	113,861	91,064	+H
Beta-Glycyrrhetinic acid	$C_{30}H_{46}O_4$	21.95	470.33961	471.3468	647,536	459,245	+H, +Na
Cyclopamine	$C_{27}H_{41}NO_2$	27.59	411.31373	412.3207	107,425	18,648	+H, +Na
Coniferin	$C_{16}H_{22}O_8$	34.22	342.13147	365.1222	13,582	13,582	+Na

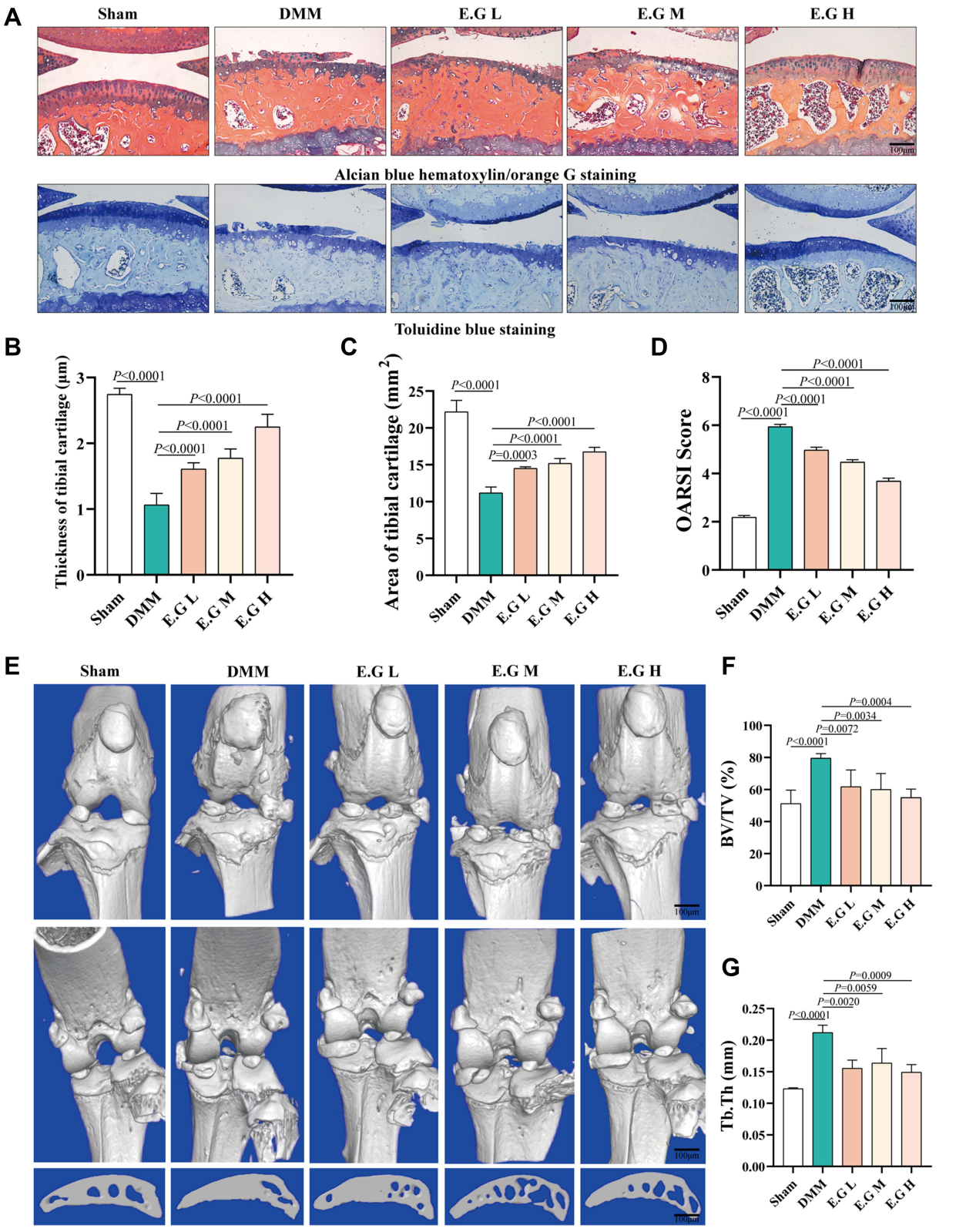

Figure 2 E.G decelerated the KOA progression in DMM-induced osteoarthritic mice. (**A**) ABH staining and TB staining of the right knee joint in C57BL/6 mice (surgical one). Morphological quantitative analysis of (**B**) area of tibial cartilage (mm^2) and (**C**) thickness of tibial cartilage (μm). (**D**) OARSI scoring of the sections analyzed by histomorphometry. (**E**) Representative 3D reconstruction of the right knee joint and subchondral bone. Scale bar=100 μm. (**F**) BV/TV (%) and (**G**) Tb.Th (mm) were quantitative analysis data of the subchondral bone. All data were taken as means ± standard deviations (n=6). The corresponding graph provided the exact *P* value.

https://doi.org/10.2147/DDDT.S397185 DovePress

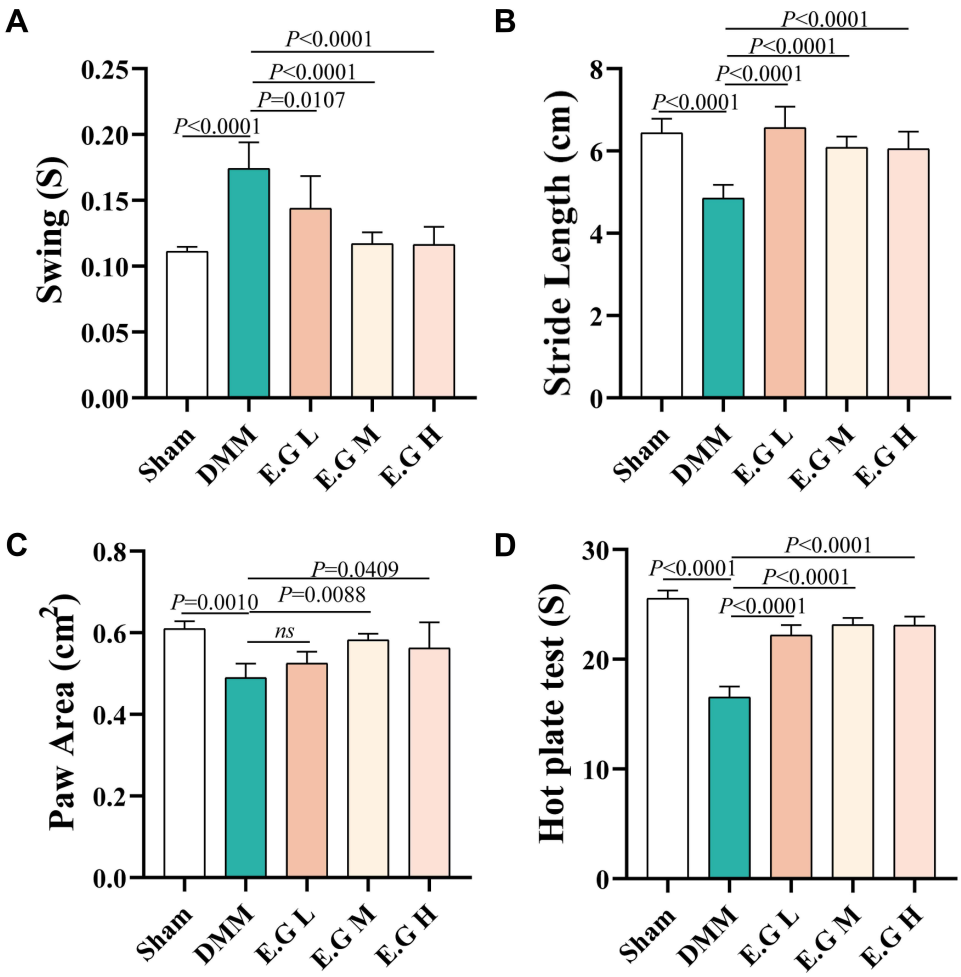

Figure 3 E.G alleviated behavioural pathological changes and pain in the DMM-induced KOA mice. (**A**) Swing (S), (**B**) Stride length (cm), (**C**) Paw area (cm^2) of the right hind limb and (**D**) hot plate reaction time (S) of mice were detected. All data were taken as means ± standard deviations (n=6). The corresponding graph provided the exact *P* value.

dependently returned these gaits and pain parameters to normal levels. Results revealed that E.G. dose-dependently enhanced the function of the knee joint and alleviated the DMM-induced gait disturbance and heat sensitivity.

E.G Inhibited Degradation of Extracellular Matrix in Osteoarthritic Articular Cartilage

In knee osteoarthritis, cartilage degeneration is primarily caused by an imbalance between anabolism and catabolism. The expression levels of Col2 and Aggrecan were representative markers of cartilage anabolic activity, and MMP13 and Adamts5 were main catabolic markers in progression of knee osteoarthritis. In this study, *immunohistochemistry* staining was performed to estimate if E.G. could modulate the levels of various markers associated with extracellular matrix metabolism in articular cartilage. The quantitative analysis results observed that in DMM-induced KOA mice, Col2 and Aggrecan were markedly downregulated, while MMP13 was considerably upregulated. E.G. reversed the trend by increasing Col2 and Aggrecan expression in cartilage and diminishing MMP13 levels of chondrocytes in a dose-dependent manner (Figure 4A–D). Above findings suggested that E.G. could secure cartilage against degradation in vivo. We explored the protective effect of E.G. on extracellular matrix degradation in chondrocytes. Altered concentrations of EGS (10%, 20%, 40%) and IL-1β (10 ng/mL) were used to co-treat primary chondrocytes for 24 h and the mRNA levels of *Col2, Aggrecan, MMP13, Adamts5* were detected. As shown in Figure 4E–H, the down-regulated with *Col2, Aggrecan* mRNA and up-regulated with *MMP13, Adamts5* induced by IL-1β were restored with the treatment of EGS, which was consistent with the histological staining experiments. Overall, these results demonstrate

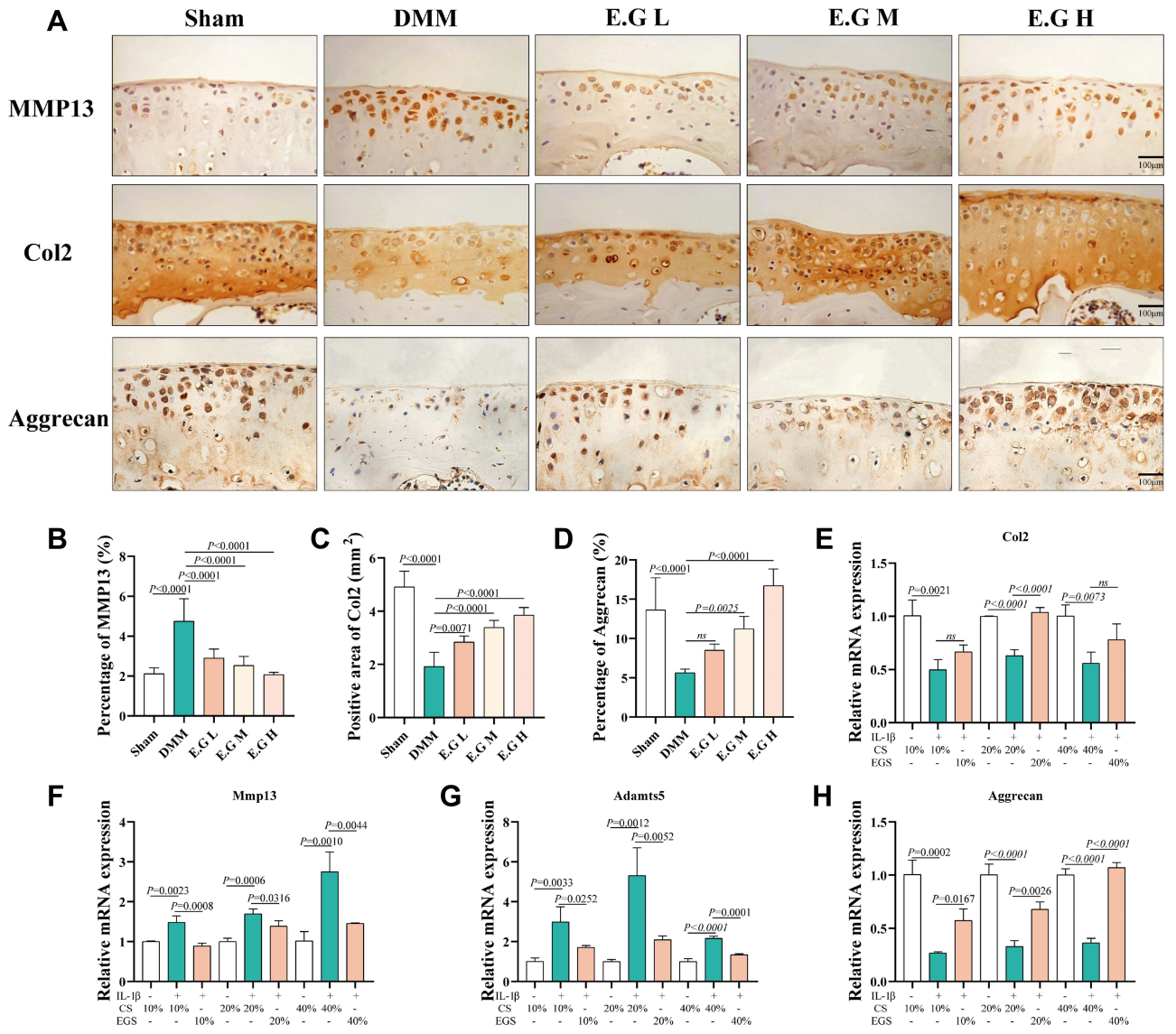

Figure 4 E.G inhibited degradation of extracellular matrix in osteoarthritic articular cartilage. (**A**) Immunohistochemical staining of MMP13, Col2 and Aggrecan in cartilage. Scale bar=100 μm. (**B–D**) Quantification of the positive repression area of Col2 (mm^2), Percentage of positive expression of MMP13 (%) and Aggrecan (%). (**E–H**) Relative mRNA expression of *Col2, Mmp13, Aggrecan* and *Adamts5* of IL-1β-induced primary mice chondrocytes treated with EGS. All data were taken as means ± standard deviations (n=6). The corresponding graph provided the exact *P* value.

that E.G. could protect against progressive knee-osteoarthritis-like degeneration of articular cartilage following DMM surgery, which might be through inhibition degradation of extracellular matrix.

Identifying E.G Targets Against KOA

The Traditional Chinese Medicine Systems Pharmacology Database and Analysis Platform (TCMSP) yielded 112 drug targets after removing duplicates, while a total of 3825 targets related to KOA were obtained from the GeneCards, OMIM, PharmGkb, TTD and Drugbank databases (Figure 5A). By comparing drug targets with KOA-related targets, we identified 61 probable targets of E.G. that contribute to the treatment of KOA (Figure 5B). There were 86 nodes and 247 edges in the protein–protein interaction (PPI) network. The average node degree was 5.744 (Figure 5C). As shown in Figure 5D, the degree above the median value was selected for visualization. Top 10 targets were PPARG, TGFβ1, STAT1, FOS, MAPK1, RELA, AKT1, PPARA and JUN, suggesting that they have a critical role in the treatment of KOA, and PPARG was the hub protein.

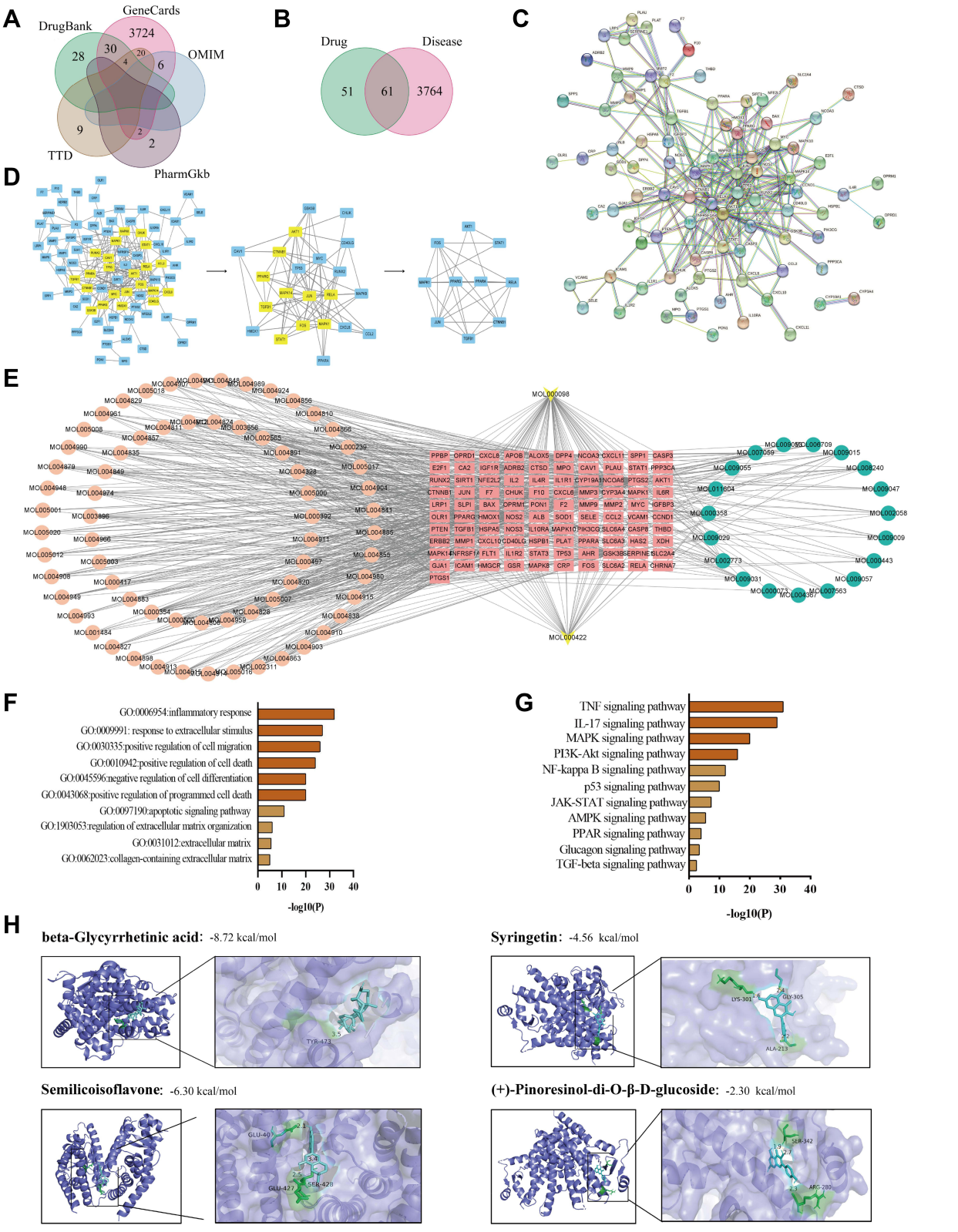

Figure 5 Network pharmacology and molecular docking analysis. (**A**) KOA's disease target overlaps between the GeneCards, OMIM, PharmGkb, TTD and Drugbank database. (**B**) Overlaps between KOA's targets and E.G drug targets. (**C**) PPI network and (**D**) core target screening. (**E**) E.G-target-KOA network. The circular node represents the traditional Chinese medicine component, the rectangular node represents the disease target, and the arrow node represents the common component of the two drugs. (**F**) GO enrichment analysis and (**G**) KEGG pathways enrichment analysis. (**H**) Molecular docking revealed the binding of beta-Glycyrrhetinic acid, syringetin, (+)-Pinoresinol-di-O-β-D-glucoside and semilicoisoflavone to PPARG protein.

Interestingly, the compounds corresponding to these targets were also identified in UPLC-Q-TOF/MS, such as naringenin, kaempferol and beta-Glycyrrhetinic acid. As shown in Figure 5E, the network consists of 190 nodes (active components and corresponding targets) and 793 edges (interactive relationship between active components and target proteins). Among them, the circular node represents the traditional Chinese medicine component, the rectangular node represents the disease target, and the arrow node represents the coarse component of the two drugs. GO and KEGG results suggested that E.G. could regulate extracellular matrix and inflammatory response to treat KOA, which might be through PI3K/AKT, NF-kappa B and PPAR signaling pathways (Figure 5F and G). Surprisingly, molecular docking analysis revealed that 10 active ingredients of E.G. could be bound to PPARG protein, such as beta-Glycyrrhetinic acid, syringetin, (+)-Pinoresinol-di-O-β-D-glucoside and semilicoisoflavone (Figure 5H). Detailed information of hydrogen-bonding interaction sites between active ingredients of E.G. and PPARG protein are illustrated in Supplemental Table S3 and Figure S1. The above bioinformatics analysis pointed out that the curative effect of E.G. on the pathological process of KOA might be closely related to PPARG.

E.G Regulated Chondrocytes Extracellular Matrix Metabolism in a PPARG-Dependent Manner

For the purpose of verifying network pharmacologic predictions, we investigated the effects of PPARG (encoded by *PPARG* gene) on the regulation of chondrocytes matrix metabolism by E.G. Firstly, immunohistochemistry results indicated that the positive expression level of PPARG in DMM model mice was seriously decreased, which was improved after E.G. treatment (Figure 6A and B). This was in agreement with our in vitro results that the decreased expression of *PPARG* mRNA induced by IL-1β was

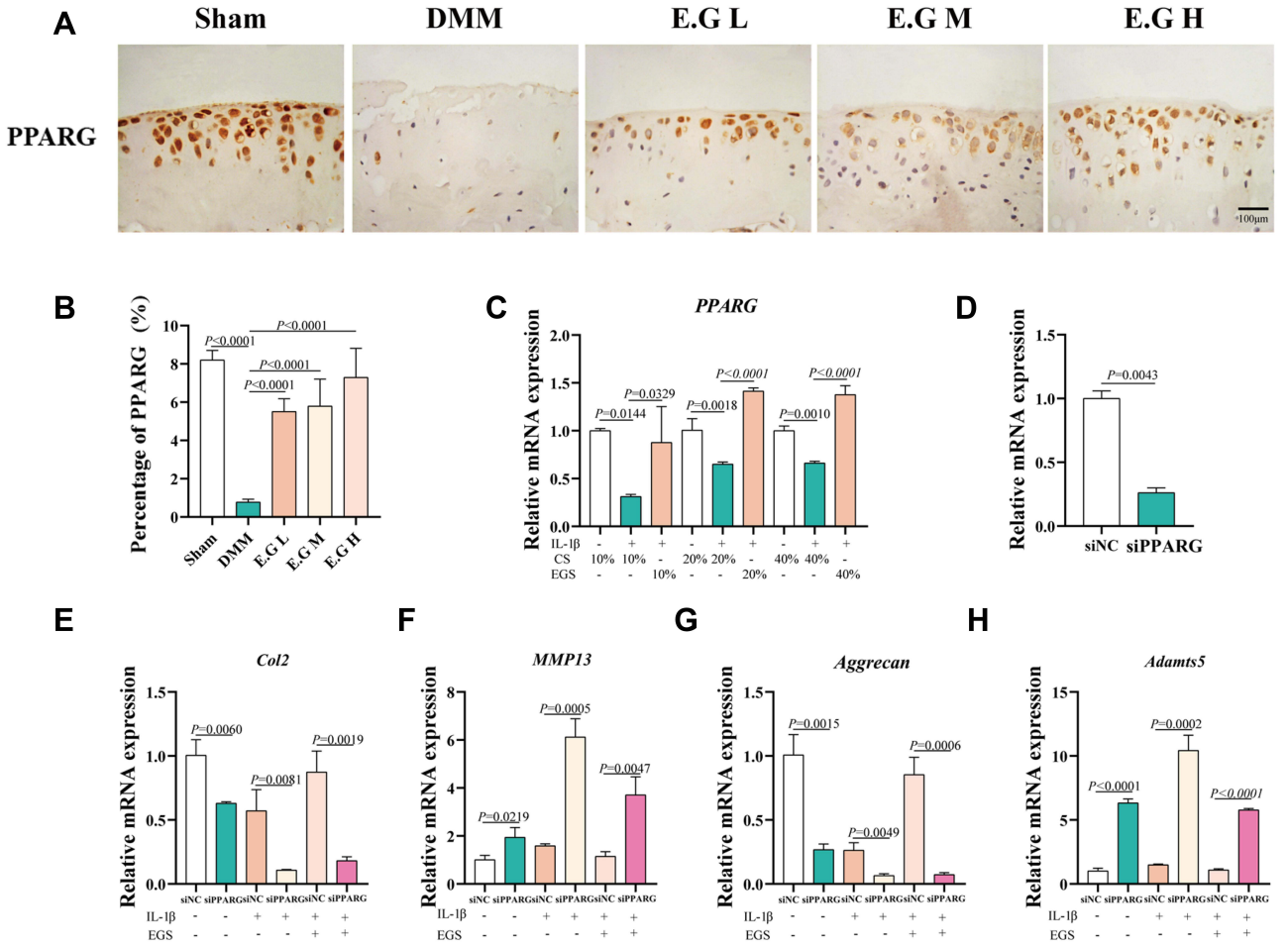

Figure 6 E.G regulated the synthesis and catabolism of chondrocytes in a PPARG-dependent manner. (**A**) Immunohistochemical staining of PPARG in cartilage. Scale bar=100 μm. (**B**) Quantification of the percentage of positive expression of PPARG (%). (**C**) Relative mRNA expression of *PPARG* in IL-1β-induced primary chondrocytes treated with EGS. (**D**) The transfection efficiency of siPPARG. (**E**–**H**) The mRNA expression of *Col2, Aggrecan, MMP13, Adamts5*. The primary mice chondrocytes were transfected for 48h and then treated with drug-containing serum for 24h. All data were taken as means ± standard deviations (n=6). The corresponding graph provided the exact *P* value.

reversed by EGS at different concentrations (Figure 6C). To elucidate the role of PPARG in cartilage of KOA, we observed extracellular matrix metabolism changes in chondrocytes by knocking down the level of *PPARG*. Unsurprisingly, chondrocytes transfected with siPPARG demonstrated significantly decreasing levels of *Col2, Aggrecan* and increasing levels of *MMP13, Adamts5* (Figure 6D–H). As expected, the silence of *PPARG* abolished the reversed effect of EGS on the anabolic genes (*Col2, Aggrecan*) and catabolic genes (*MMP13, Adamts5*) of chondrocyte extracellular matrix (Figure 6D–H). Based on these findings, E.G. may partially protect chondrocyte extracellular matrix metabolism via PPARG.

Discussion

Inflammation and mechanical loading are important pathogenic factors involved in the pathogenesis of KOA.[27,28] Until now, approved disease-modifying KOA drugs continue to be lacking. In the present study, we demonstrated that E.G. couplet medicines significantly ameliorated KOA development by regulating articular cartilage anabolic/catabolic homeostasis to prevent cartilage degeneration and improving abnormal behavior and pain parameters. Subsequently, we have identified the principal active ingredients via UPLC-Q-TOF/MS, and systematically analysed the targets and effective signaling pathways highly relevant to E.G. through network pharmacology analysis and in vitro study.

Traditional Chinese Medicine (TCM) is becoming an essential medical option for KOA. It is worth noting that TCM couplet medicines are widely used in diseases, which can exert synergistic and cascading effects. In this study, *Eucommia ulmoides* Oliv. and *Glycyrrhiza uralensis* Fisch. (E.G.) couplet medicines were chosen to treat KOA. They are precious traditional Chinese medicinal plants having a long history of medicinal use and commonly used in clinical practice. *Eucommia ulmoides* Oliv. is an important warming and toxifying kidney-yang herb for the treatment of waist and knee pain, joint disadvantage and muscle and bone weakness.[29–31] *Glycyrrhiza uralensis* Fisch. is a qi-invigorating herb, which has been proven to enhance the functions of immunity, anti-inflammatory, anti-gastric ulcer, anti-arrhythmia and regulate blood glucose.[32–34] Although the potential anti-KOA effects of *Eucommia ulmoides* Oliv. and *Glycyrrhiza uralensis* Fisch. have been, respectively, reported,[35,36] energetic ingredients and exact mechanism of E.G. are still unclear.

Here, we confirmed that E.G. could dose-dependently inhibit prominent local articular cartilage damage, cartilage area and decreased thickness in DMM-induced KOA mice, as well as the formation of osteophytes and subchondral bone sclerosis of the knee joint. Mechanical loading and inflammation stimulation can promote excessive catabolic processes in articular cartilage, driving the formation of KOA.[37,38] E.G. could prevent articular cartilage extracellular matrix degradation through promoting articular cartilage anabolism (increasing Col2, Aggrecan levels) and restraining catabolism (decreasing MMP13, Adamts5 levels). Knee joint mobility limitation and joint pain are the most obvious clinical manifestations of KOA patients.[39,40] Excitingly, our results showed that E.G. enhanced knee joint function alleviated gait disturbances and heat sensitivity in KOA mice. Subsequently, we identified the main active ingredients via UPLC-Q-TOF/MS, and comprehensively analysed targets and potential pathways highly related to E.G. through network pharmacology analysis. Top 10 targets were candidates thought to be highly correlated with KOA, including PPARG, TGFβ1, STAT1, FOS, MAPK1, RELA, AKT1, PPARA, JUN and PPARG as the hub protein. GO and KEGG analysis showed that E.G. might focus on PI3K/AKT, NF-kappa B and PPAR signaling pathways to regulate extracellular matrix and inflammatory response. In addition, molecular docking analysis excavated 10 active ingredients of E.G. binding to PPARG protein, suggesting that PPARG might be a key target of E.G. to prevent KOA.

PPARG belongs to the nuclear hormone receptor superfamily and plays a critical role in inflammation-related diseases. Previous studies indicated that PPARG reduction in osteoarthritic cartilage was highly correlated with increased expression of inflammatory and catabolic factors.[41–43] To further validate the results of network pharmacological analysis, we first confirmed that the level of PPARG in articular cartilage of DMM-induced mice was reduced significantly, which could be rescued with E.G. treatment. Similarly, an in vitro study showed that EGS could up-regulate *PPARG* mRNA level in IL-1β-treated chondrocytes. Interestingly, the effects of EGS on the increment of anabolic gene expression (*Col2, Aggrecan*) and the decrement of catabolic gene expression (*MMP13, Adamts5*) of chondrocyte extracellular matrix was abolished due to the silence of *PPARG*. These results demonstrated that PPARG was necessary for the regulation of E.G. on articular cartilage anabolic/catabolic homeostasis required the presence of

PPARG. However, additional studies are still necessary to explicitly explain the specific mechanisms of PPARG and explore the exact individual ingredients of E.G. in the treatment of KOA.

In conclusion, we integrated UPLC-Q-TOF/MS, network pharmacology analysis and experimental evidence to elucidate the anti-KOA mechanism of E.G. by inhibiting the articular cartilage degradation to protect chondrocytes through PPARG, which might be a potential therapeutic target of E.G. for KOA treatment.

Abbreviations

E.G., *Eucommia ulmoides* Oliv.-*Glycyrrhiza uralensis* Fisch.; KOA, Knee osteoarthritis; DMM, destabilization of the medial meniscus; EGS, E.G.-containing serum; CS, control serum; GO, Gene Ontology; KEGG, Kyoto Encyclopaedia of Genes and Genomes; Col2, type II collagen; MMP13, matrix metalloproteinase 13; PPARG, peroxisome proliferator-activated receptor gamma; TCM, Traditional Chinese medicine; UPLC-Q-TOF/MS, Ultra performance liquid chromatography and quadrupole/time-of-flight mass spectrometry.

Acknowledgments

The Public Platform of Medical Research Center, Academy of Chinese Medical Science, Zhejiang Chinese Medical University has provided excellent technical support.

Author Contributions

All authors made a significant contribution to the work reported, whether that is in the conception, study design, execution, acquisition of data, analysis and interpretation, or in all these areas; took part in drafting, revising or critically reviewing the article; gave final approval of the version to be published; have agreed on the journal to which the article has been submitted; and agree to be accountable for all aspects of the work.

Funding

This study was partially supported by Natural Science Foundation of China (Grant no. 81973869 and 82104889), Zhejiang Provincial Natural Science Foundation of China (Grant no. LY22H270005), the State Administration of Traditional Chinese Medicine of Zhejiang Province (Grant no. 2021ZZ014), the Research Project of Zhejiang Chinese Medical University (Grant no. 2022JKZKTS32).

Disclosure

The authors have declared that no conflict of interest exists.

References

1. Vina ER, Kwoh CK. Epidemiology of osteoarthritis: literature update. *Curr Opin Rheumatol*. 2018;30:160–167. doi:10.1097/BOR.0000000000000479
2. Hunter DJ, Bierma-Zeinstra S. Osteoarthritis. *Lancet*. 2019;393:1745–1759. doi:10.1016/S0140-6736(19)30417-9
3. Roos EM, Arden NK. Strategies for the prevention of knee osteoarthritis. *Nat Rev Rheumatol*. 2016;12(2):92–101. doi:10.1038/nrrheum.2015.135
4. Wallace IJ, Worthington S, Felson DT, et al. Knee osteoarthritis has doubled in prevalence since the mid-20th century. *Proc Natl Acad Sci U S A*. 2017;114(35):9332–9336. doi:10.1073/pnas.1703856114
5. Scanzello CR. Role of low-grade inflammation in osteoarthritis. *Curr Opin Rheumatol*. 2017;29(1):79–85. doi:10.1097/BOR.0000000000000353
6. Glyn-Jones S, Palmer AJ, Agricola R, et al. Osteoarthritis. *Lancet*. 2015;386(9991):376–387. doi:10.1016/S0140-6736(14)60802-3
7. Shen J, Abu-Amer Y, O'Keefe RJ, McAlinden A. Inflammation and epigenetic regulation in osteoarthritis. *Connect Tissue Res*. 2017;58(1):49–63. doi:10.1080/03008207.2016.1208655
8. Meliconi R, Pulsatelli L. Are mechanisms of inflammation joint-specific in osteoarthritis? *Rheumatology*. 2019;58(5):743–745. doi:10.1093/rheumatology/key300
9. van den Bosch MHJ. Osteoarthritis year in review 2020: biology. *Osteoarthritis Cartilage*. 2021;29(2):143–150. doi:10.1016/j.joca.2020.10.006
10. Robinson WH, Lepus CM, Wang Q, et al. Low-grade inflammation as a key mediator of the pathogenesis of osteoarthritis. *Nat Rev Rheumatol*. 2016;12:580–592. doi:10.1038/nrrheum.2016.136
11. Rannou F, Pelletier JP, Martel-Pelletier J. Efficacy and safety of topical NSAIDs in the management of osteoarthritis: evidence from real-life setting trials and surveys. *Semin Arthritis Rheum*. 2016;45:S18–S21. doi:10.1016/j.semarthrit.2015.11.007
12. Bijlsma JW, Berenbaum F, Lafeber FP. Osteoarthritis: an update with relevance for clinical practice. *Lancet*. 2011;377:9783. doi:10.1016/S0140-6736(11)60243-2
13. Martel-Pelletier J, Barr AJ, Cicuttini FM, et al. Osteoarthritis. *Nat Rev Dis Primers*. 2016;2:16072. doi:10.1038/nrdp.2016.72
14. Hammaker D, Firestein GS. Epigenetics of inflammatory arthritis. *Curr Opin Rheumatol*. 2018;30:188–196. doi:10.1097/BOR.0000000000000471

15. Sharma L, Solomon CG. Osteoarthritis of the Knee. *N Engl J Med*. 2021;384:51–59. doi:10.1056/NEJMcp1903768
16. Wang CY, Tang L, He JW, Li J, Wang YZ. Ethnobotany, phytochemistry and pharmacological properties of eucommia ulmoides: a review. *Am J Chin Med*. 2019;47:259–300. doi:10.1142/S0192415X19500137
17. Zhu MQ, Sun RC. Eucommia ulmoides Oliver: a potential feedstock for bioactive products. *J Agric Food Chem*. 2018;66:5433–5438. doi:10.1021/acs.jafc.8b01312
18. Sultan MT, Butt MS, Qayyum MM, Suleria HA. Immunity: plants as effective mediators. *Crit Rev Food Sci Nutr*. 2014;54:1298–1308. doi:10.1080/10408398.2011.633249
19. Yang R, Yuan BC, Ma YS, Zhou S, Liu Y. The anti-inflammatory activity of licorice, a widely used Chinese herb. *Pharm Biol*. 2017;55:5–18. doi:10.1080/13880209.2016.1225775
20. Wang PE, Zhang L, Ying J, et al. Bushenhuoxue formula attenuates cartilage degeneration in an osteoarthritic mouse model through TGF-beta/MMP13 signaling. *J Transl Med*. 2018;16(72). doi:10.1186/s12967-018-1437-3
21. Sun Z, Su W, Wang L, Cheng Z, Yang F. Clinical effect of bushen huoxue method combined with platelet-rich plasma in the treatment of knee osteoarthritis and its effect on IL-1, IL-6, VEGF, and PGE-2. *J Healthc Eng*. 2022;2022:9491439. doi:10.1155/2022/9491439
22. Liu L, Xu L, Wang S, et al. Confirmation of inhibitingTLR4/MyD88/NF-kappaB signalling pathway by duhuo jisheng decoction on osteoarthritis: a network pharmacology approach-integrated experimental study. *Front Pharmacol*. 2021;12:784822. doi:10.3389/fphar.2021.784822
23. Wu G, Chen W, Fan H, et al. Duhuo Jisheng Decoction promotes chondrocyte proliferation through accelerated G1/S transition in osteoarthritis. *Int J Mol Med*. 2013;32:1001–1010. doi:10.3892/ijmm.2013.1481
24. Kim BJ, Kim DW, Kim SH, et al. Establishment of a reliable and reproducible murine osteoarthritis model. *Osteoarthritis Cartilage*. 2013;21:2013–2020. doi:10.1016/j.joca.2013.09.012
25. Liu X, Chai Y, Liu G, et al. Osteoclasts protect bone blood vessels against senescence through the angiogenin/plexin-B2 axis. *Nat Commun*. 2021;12:1832. doi:10.1038/s41467-021-22131-1
26. Blakely CM, Watkins TBK, Wu W, et al. Evolution and clinical impact of co-occurring genetic alterations in advanced-stage EGFR-mutant lung cancers. *Nat Genet*. 2017;49:1693–1704. doi:10.1038/ng.3990
27. Ter Heegde F, Luiz AP, Santana-Varela S, et al. Osteoarthritis-related nociceptive behaviour following mechanical joint loading correlates with cartilage damage. *Osteoarthritis Cartilage*. 2020;28:383–395. doi:10.1016/j.joca.2019.12.004
28. Goldring MB, Otero M. Inflammation in osteoarthritis. *Curr Opin Rheumatol*. 2011;23(5):471–478. doi:10.1097/BOR.0b013e328349c2b1
29. Sun Y, Huang K, Mo L, et al. Eucommia ulmoides polysaccharides attenuate rabbit osteoarthritis by regulating the function of macrophages. *Front Pharmacol*. 2021;12:730557. doi:10.3389/fphar.2021.730557
30. Huang L, Lyu Q, Zheng W, Yang Q, Cao G. Traditional application and modern pharmacological research of Eucommia ulmoides Oliv. *Chin Med*. 2021;16(1). doi:10.1186/s13020-021-00482-7
31. Kim JY, Lee JI, Song M, et al. Effects of Eucommia ulmoides extract on longitudinal bone growth rate in adolescent female rats. *Phytother Res*. 2015;29(1):148–153. doi:10.1002/ptr.5195
32. Chen B, Zhu D, Xie C, et al. 18beta-Glycyrrhetinic acid inhibits IL-1beta-induced inflammatory response in mouse chondrocytes and prevents osteoarthritic progression by activating Nrf2. *Food Funct*. 2021;12(18):8399–8410. doi:10.1039/d1fo01379c
33. Liu Y, Zhang M, Cheng J, et al. Novel carbon dots derived from glycyrrhizae radix et rhizoma and their anti-gastric ulcer effect. *Molecules*. 2021;26. doi:10.3390/molecules26061512
34. Ferrari P. Licorice: a sweet alternative to prevent hyperkalemia in dialysis patients? *Kidney Int*. 2009;76(8):811–812. doi:10.1038/ki.2009.282
35. Zhao L, Chen X, Shao X, et al. Prenylated phenolic compounds from licorice (Glycyrrhiza uralensis) and their anti-inflammatory activity against osteoarthritis. *Food Funct*. 2022;13:795–805. doi:10.1039/d1fo03659a
36. Xie GP, Jiang N, Wang SN, et al. Eucommia ulmoides Oliv. bark aqueous extract inhibits osteoarthritis in a rat model of osteoarthritis. *J Ethnopharmacol*. 2015;162:148–154. doi:10.1016/j.jep.2014.12.061
37. Hodgkinson T, Kelly DC, Curtin CM, O'Brien FJ. Mechanosignalling in cartilage: an emerging target for the treatment of osteoarthritis. *Nat Rev Rheumatol*. 2022;18(2):67–84. doi:10.1038/s41584-021-00724-w
38. Grandi FC, Baskar R, Smeriglio P, et al. Single-cell mass cytometry reveals cross-talk between inflammation-dampening and inflammation-amplifying cells in osteoarthritic cartilage. *Sci Adv*. 2020;6:eaay5352. doi:10.1126/sciadv.aay5352
39. Sanada Y, Tan SJO, Adachi N, Miyaki S. Pharmacological targeting of heme oxygenase-1 in osteoarthritis. *Antioxidants*. 2021;10(3):419. doi:10.3390/antiox10030419
40. Kanavaki AM, Rushton A, Efstathiou N, et al. Barriers and facilitators of physical activity in knee and Hip osteoarthritis: a systematic review of qualitative evidence. *BMJ Open*. 2017;7(12):e017042. doi:10.1136/bmjopen-2017-017042
41. Zhu X, Chen F, Lu K, Wei A, Jiang Q, Cao W. PPARγ preservation via promoter demethylation alleviates osteoarthritis in mice. *Ann Rheum Dis*. 2019;78(10):1420–1429. doi:10.1136/annrheumdis-2018-214940
42. Lu J, Guan H, Wu D, et al. Pseudolaric acid B ameliorates synovial inflammation and vessel formation by stabilizing PPARgamma to inhibit NF-kappaB signalling pathway. *J Cell Mol Med*. 2021;25(14):6664–6678. doi:10.1111/jcmm.16670
43. Ni S, Li D, Wei H, Miao KS, Zhuang C. PPARgamma attenuates interleukin-1beta-induced cell apoptosis by inhibiting NOX2/ROS/p38MAPK activation in osteoarthritis chondrocytes. *Oxid Med Cell Longev*. 2021;2021:5551338. doi:10.1155/2021/5551338